SOLID STATE ^{13}C RELAXATION STUDIES OF COALS

R. E. Botto* and David E. Axelson**

*Chemistry Division, Argonne National Laboratory,
9700 South Cass Avenue, Argonne, IL 60439

**Energy, Mines & Resources Canada, CANMET,
P.O. Box 1280, Devon, Alberta, Canada TOC 1EO

INTRODUCTION

Despite many studies of coal and related fossil fuels, no attempts have been made to systematically correlate changes in the solid state ^{13}C-NMR parameters as a function of static field strength. In particular, questions arise regarding differences in spectral resolution and relaxation parameters. While discrimination among the complex structural components of fossil fuels can be based on relaxation time differences (1), this also necessitates a more intensive study of static field-strength effects if a more complete understanding of coal structure is to be gained.

Carbon-13 spin-lattice relaxation was chosen as the parameter of interest for this study because it represents a "dilute" nuclear spin system, which therefore minimizes spin diffusion interaction among phases. Furthermore, it is not as complicated to interpret as $T_{1\rho}$ measurements, and exhibits a field dependence in the slow motion regime (Figure 1). These studies also comprise part of a more comprehensive on-going evaluation of the Argonne Premium Coal Samples.

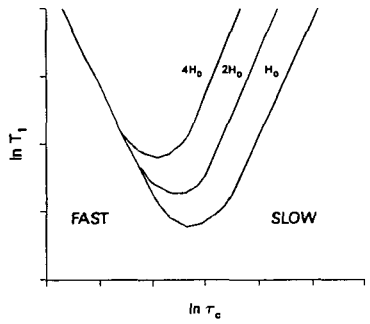

Figure 1. Motional dependence of T_1 with magnetic field.

EXPERIMENTAL

All NMR spectra taken at higher field were obtained on a Bruker CXP-200 spectrometer. Parameters used to acquire data were as follows: spectrometer frequency 50.306 MHz, 3 kHz magic-angle spinning in a boron nitride rotor containing a deuterated polymethylmethacrylate base (exhibiting no ^{13}C background from residual non-deuterated material), dipolar decoupling of 50-60 kHz, 90° pulse width of 4-5 ms, spin temperature alternation of the H-1 pulse, 20 kHz spectral width, 4K data points, 50-75 Hz line broadening, 500-3000 scans/spectrum, ambient temperature, 12 bit digitizer resolution, quadrature detection, both normal and spinning-sideband suppressed spectra (TOSS), recycle delay 3-5 s, contact time 1 ms and 50-80 ms decoupling time. All chemical shifts were reference to TMS via adamantane as a secondary reference.

Spectra taken at lower field at Argonne were obtained at 25.18 MHz using a Bruker CXP-100 spectrometer in the pulse Fourier transform mode with quadrature phase detection. The sample spinners were made of ceramic with an internal volume of 250 μL and were spun at approximately 4 kHz. Operating parameters in CP experiments included a spectra width of 10 kHz, a 90° proton pulse width of 3.75 μs (67-kHz proton-decoupling field), an acquisition time of 20 ms, a pulse repetition time of 2s, a contact time of 1.5 ms, and a total accumulation of 1000 transients. In a typical experiment, words of memory were allocated for data acquisition and then increased to 4K (2K real data) by zero filling. Before Fourier transformation of the data, the interferogram was multiplied by a decreasing trapezoidal window function after the first 40 data points. Carbon aromaticities were derived from integrated signal intensities for sp^2-hybridized (δ 110-160) and sp^3-hybridized (δ 0-60) carbon absorption bands. For the aromatic carbons, signal intensities of the spinning sidebands were added to the intensity of the centerband. Chemical shifts were referenced to TMS using tetrakis(trimethylsilyl)silane [TKS] as a secondary reference (2).

American coals were obtained from the Argonne Premium Coal Sample Program. For the Canadian coals, homogenized bulk samples representative of the coal deposits from their respective regions were obtained by a bucket auger drill rig. Samples were stored in sealed barrels at low temperatures to minimize long term deterioration. The same samples were used for the NMR measurements on the two instruments to eliminate sample heterogeneity problems for the purposes of this comparison.

RESULTS AND DISCUSSION

Proximate and ultimate analysis of the coals are summarized in Table 1. Apparent aromaticities are given in Table 2 and carbon-13 spin-lattice relaxation measurements are shown in Table 3.

Related studies on proton relaxation at different fields have been reported by Packer et al. (3), Pembleton (4), and Sullivan et al. (5). Dudley and Fyfe (6) discussed carbon relaxation times for a pitch and three Canadian coals. Emphasis was placed on the effects of paramagnetics (including oxygen) in rationalizing the results. Palmer and Maciel (7) reported relaxation parameters for a kerogen concentrate of a Colorado oil shale and Powhatan #5 coal. Aliphatic and aromatic regions exhibited bi-exponential relaxation decay curves for both T_1 and T_2 measurements for the kerogen concentrate. The coal sample was characterized by T_{1C} of 5.8 s for all carbons (B_0 = 1.4 T, 21°C). For the kerogen concentrate the effect of the static field strength on the T_{1H} value was also determined. On increasing B_0 from 1.4 T to 4.7 T the proton T_1 increased from about 100 ms to 184 ms. Changing the temperature from ambient to -141C resulted in only a marginal increase in T_1 to 124 ms, whereas the optimum contact time did not change at all.

Figure 2 illustrates the nature of the spectra obtained on a low rank coal (lignite) at the two different field strengths. The 50-MHz CP/MAS spectrum was obtained using sideband suppression (TOSS). No apparent differences in resolution exist under these conditions.

Apparent aromaticities are summarized in Table 2. The average deviation for the ten coals at the two fields is about ±0.02 units, about equal to the precision

TABLE 1. Ultimate Analysis of Coals.[a]

Sample	C	H	N	O	S	A
Beulah-Zap lignite (APCS #8)	72.9	4.83	1.15	20.30	0.70	9.7
Wyodak-Anderson subB (APCS #2)	75.0	5.35	1.12	18.00	0.47	8.8
Herrin hvCB (APCS #3)	77.7	5.00	1.37	13.50	2.38	15.5
Upper Freeport mvB (APCS #1)	85.5	4.70	1.55	13.20	0.74	13.2
Pocahontas lvB (APCS #5)	91.0	4.44	1.33	2.47	0.50	4.2
Ontario lignite	66.9	4.65	0.9	27.23	0.32	4.8
Ardley subB	75.7	4.1	1.2	18.5	0.50	20.0
Smokey Tower subB	75.8	5.1	1.7	16.9	0.50	20.0
Dunvegan hvAB	84.4	5.6	2.1	5.4	2.50	4.4
Gates lvB	93.2	4.63	1.5	0.17	0.50	11.0

[a]Column headings defined as follows: C = % carbon; H = % hydrogen, N = % nitrogen; O = % oxygen; S = % sulfur; A = ash.

TABLE 2. Apparent Carbon Aromaticities of Coals.

Coal	Aromaticity	
	2.3 Tesla CP/MAS	4.7 Tesla TOSS
Beulah-Zap lignite	0.66	0.69
Ontario lignite	0.62	0.61
Wyodak-Anderson subbituminous	0.67	0.63
Ardley subbituminous B	0.74	0.75
Smokey Tower subbituminous A	0.66	0.67
Herrin hvC bituminous	0.72	0.71
Dunvegan hvA bituminous	0.76	0.71
Upper Freeport mv bituminous	0.82	0.81
Pocahontas lv bituminous	0.85	0.86
Gates lv bituminous	0.82	0.82

TABLE 3. Carbon T_1(s) Relaxation in Coals.

Coal	2.3 Tesla		4.7 Tesla	
	Aliphatic	Aromatic	Aliphatic	Aromatic
Beulah-Zap lignite	0.3 (34%)	0.3 (46%)	0.1 (54%)	0.1 (57%)
(APCS #8)	1.7 (66%)	2.4 (54%)	1.9 (46%)	2.0 (43%)
Ontario lignite	0.6 (68%)	0.8 (58%)	0.2 (41%)	0.2 (46%)
	6.7 (32%)	4.7 (42%)	3.3 (59%)	5.0 (54%)
Wyodak-Anderson subbituminous	0.8 (38%)	0.9 (36%)	0.4 (67%)	0.2 (63%)
(APCS #2)	2.1 (62%)	2.2 (64%)	7.5 (33%)	6.0 (37%)
Ardley subbituminous B	---	---	0.6 (45%)	0.7 (46%)
	1.2	1.4	3.0 (55%)	5.2 (54%)
Smokey Tower subbituminous A	0.6 (41%)	0.5 (35%)	0.3 (72%)	0.3 (65%)
	1.2 (59%)	1.6 (65%)	6.1 (28%)	4.5 (35%)
Illinois No. 6 hv bituminous	1.4 (38%)	3.0 (34%)	0.1 (39%)	0.1 (24%)
(APCS #3)	5.5 (62%)	9.9 (65%)	9.2 (61%)	14.7 (76%)
Dunvegan hvA bituminous	3.0 (37%)	6.2 (25%)	0.9 (48%)	---
	5.8 (63%)	13.9 (75%)	22.3 (52%)	25.3
Upper Freeport mv bituminous	1.2 (60%)	9.0 (9%)	1.5 (38%)	---
(APCS #1)	6.9 (40%)	10.2 (91%)	14.8 (62%)	20.6
Pocahontas lv bituminous	---	4.7 (17%)	0.3 (18%)	0.1 (6%)
(APCS #5)	5.6	9.1 (83%)	10.7 (82%)	15.7 (94%)
Gates lv bituminous	---	---	0.4 (38%)	---
	3.5	5.9	9.3 (62%)	15.5

of the aromaticity measurements. The effects of sideband suppression and magic-angle spinning itself on aromaticity measurements of fossil fuels have been discussed previously (8,9). Agreement is reasonably good between aromaticities derived from both normal and sideband suppressed spectra for this series.

More significant deviations in measured aromaticities arise from comparison of values derived from spinning and non-spinning samples (9-12). Line narrowing is found in the strong collision limit ($\omega t >> 1$) due to effective coherent spatial averaging from magic-angle spinning, as well as in the weak collision limit ($\omega t << 1$) due to incoherent averaging from the random molecular motion. In the intermediate regime ($\omega t = 1$), where the MAS frequencies are similar to the frequencies associated with the molecular motion of either some or all components of the sample, destructive interference gives rise to severely broadening lines. This phenomenon occurs over a relatively narrow range of spinning frequencies (10,11). A similar destructive interference effect has also been noted between dipolar decoupling frequencies and molecular motion (12). Subject to these considerations, the present data indicate that good agreement can be attained in independent measurements of apparent aromaticities of spinning samples.

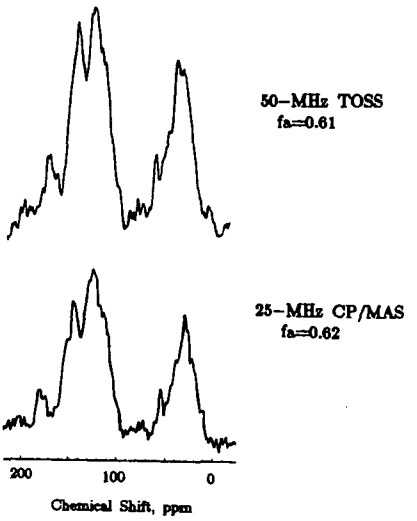

Figure 2. 25- and 50- MHz CP/MAS spectra of Ontario lignite.

The ^{13}C spin-lattice relaxation times (in seconds) and corresponding mass fractions (percentages in brackets) for all samples studied are given in Table 3. Aliphatic and aromatic regions at both field strengths were analyzed separately. Most coals exhibited two-component exponential decays for each region. Differences in relaxation times of these components vary widely (from a factor of about 2 to over 30). Separation of the decays for the more similar relaxation rates gives rise to greater uncertainty in the mass fractions reported, although trends are still discernible as a function of rank.

Figure 3 illustrates one such trend between rank (as denoted by %C) and the ^{13}C T_1 of the long component of the aromatic decay. For the low-rank coals the relaxation time for this fraction is of the order of 2-6 seconds, with the longer relaxation times usually associated with the higher field. Above the 80%C the T_1 difference at the two static field strengths increase significantly for the same sample. In addition, the relaxation times appear to reach a maximum value

at about 85%C. The phenomenon occurs at both fields. A similar trend is observed for the long relaxing component of the aliphatic carbon.

The trends in Figure 3 arise from differences in coal structure that also vary systematically with rank. These compositional variations are reflected in both the field dependence of the measurements and the observation of the maximum. We propose that these data can be related to two general factors: an underlying difference in coal structure as rank increases and the presence of paramagnetic species (oxygen, heavy metal minerals, organic free radicals). In the former case, changes in molecular motion (overall rotational diffusion, local segmental and librational motions) would be manifest as T_1 differences. In the latter instance, paramagnetic species in sufficient quantity could dramatically reduce the T_1 values measured.

A plot of the mass fraction of the long relaxing aromatic component versus %C is shown in Figure 4. At both fields there is a systematic increase in the fraction of species relaxing slowly. This trend may be attributed, in part, to a decrease in the oxygen-rich humic portion of the coals studied with increasing rank. Scatter in mass fraction measurements reflects the relative difficulty of deconvoluting overlapping decays of varying degrees of similarity (and with different signal-to-noise ratios) at the two fields.

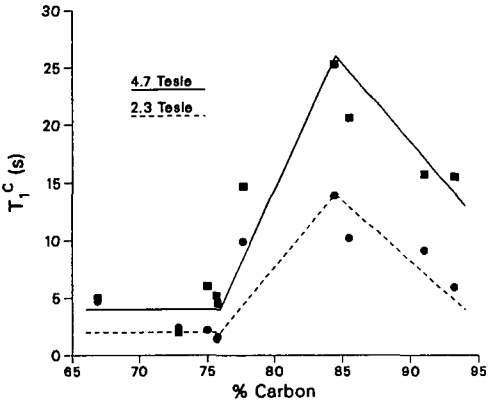

Figure 3. Variation in aromatic carbon relaxation (long) with carbon content of coal.

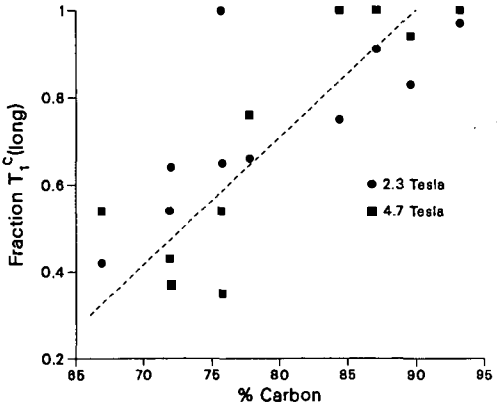

Figure 4. Variation in fraction aromatic T_1^C (long) with carbon content of coal.

As confirmation of the effect of paramagnetic species on our measurements, the Beulah-Zap lignite was treated with a dilute HCl solution to remove iron. The relaxation decay changed significantly as shown in Figure 5. The original two-component decay became a single-exponential decay after treatment, with a concomitant increase in the relaxation time occurring. Atomic absorption data on the HCl washings indicate a significant level of extractable iron in this lignite sample: 1,951 μg Fe/g coal. Relaxation discrimination experiments allow the analysis of short and long relaxing components and will be presented.

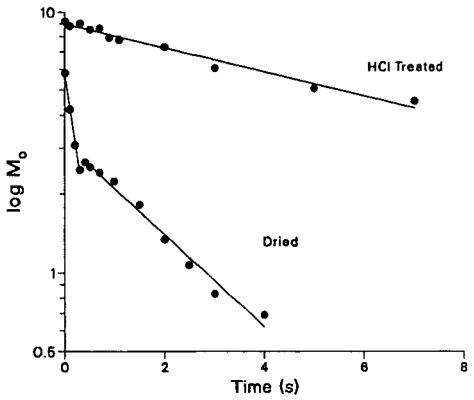

Figure 5. Changes in aromatic carbon T_1 of APCS #8 with acid treatment.

CONCLUSIONS

Spectral resolution is virtually invariant with rank over the static frequency range of 25 to 50 MHz. Although correlations between relaxation times and rank - related parameters are clearly observed at both field strengths, they probably arise from both fundamental changes in coal structure (with increasing degree of coalification) and systematic variations in the nature and extent of paramagnetic species present. The paramagnetic species themselves may represent a combination of stable organic free radicals present in large aromatic ring systems and a distribution of inorganic species, presumably which are chelated to oxygen-rich organic structures (particularly in the low-rank coals). The presence of a maximum in the spin-lattice relaxation time at both fields at 85%C probably reflects these competing interactions.

For the raw, untreated coals there are systematic differences in relaxation times with rank that may be of use in relaxation discrimination experiments.

It remains to be determined how the concentration and exact distribution of paramagnetic species can be quantitatively related to the relaxation rates observed. The rank dependence of these variables is also of ultimate concern for the rationalization of these data.

REFERENCES

1. D. E. Axelson, "Solid State NMR of Fossil Fuels", Multiscience, Montreal, 1985.
2. J. V. Muntean, L. M. Stock, R. E. Botto, J. Magn. Reson., 48, 35 (1988).
3. K. J. Packer, R. K. Harris, A. M. Kenwright, C. E. Snape, Fuel, 62, 999 (1983).
4. R. G. Pembleton, Ph.D. Thesis, Iowa State University, 1978.
5. M. J. Sullivan, N. M. Szeverenyi, G. E. Maciel, "Magnetic Resonance Introduction, Advanced Topics and Applications to Fossil Energy", L. Petrakis, J. P. Fraissard (Eds.), pp. 607-616, D. Reidel Publishing Company, 1984.
6. R. L. Dudley and C. A. Fyfe, Fuel, 61, 651 (1982).
7. A. J. Plamer and G. E. Maciel, Anal. Chem., 54, 2194 (1982).
8. R. E. Botto and R. E. Winans, Fuel, 62, 271 (1983).
9. D. E. Axelson, Fuel, 66, 195-199 (1987).
10. D. Suwelack, W. P. Rothwell, and J. S. Waugh, J. Chem. Phys., 73, 2559 (1980).
11. P. Ollivier and B. C. Gerstein, Carbon, 22, 409 (1984).
12. W. P. Rothwell and J. S. Waugh, J. Chem. Phys., 74, 2721 (1981).

ACKNOWLEDGMENT

This work was performed under the auspices of the Office of Basic Energy Sciences, Division of Chemical Sciences, U.S. Department of Energy, under contract number W-31-109-ENG-38.